

# $\Lambda N$ scattering length from the reaction $\gamma d \rightarrow K^+ \Lambda n$

A. Gasparyan<sup>1,2</sup>, J. Haidenbauer<sup>3</sup>, C. Hanhart<sup>3</sup>, and K. Miyagawa<sup>4</sup>

<sup>1</sup> Institute of Theoretical and Experimental Physics, 117259, B. Cheremushkinskaya 25, Moscow, Russia

<sup>2</sup> Gesellschaft für Schwerionenforschung (GSI), Planck Str. 1, D-64291 Darmstadt, Germany

<sup>3</sup> Institut für Kernphysik (Theorie), Forschungszentrum Jülich, D-52425 Jülich, Germany

<sup>4</sup> Simulation Science Center, Okayama University of Science, 1-1 Ridai-cho, Okayama 700-0005, Japan

Received: date / Revised version: date

**Abstract.** The prospects of utilizing the strangeness-production reaction  $\gamma d \rightarrow K^+ \Lambda n$  for the determination of the  $\Lambda n$  low-energy scattering parameters are investigated. The spin observables that need to be measured in order to isolate the  $\Lambda n$  singlet ( $^1S_0$ ) and triplet ( $^3S_1$ ) states are identified. Possible kinematical regions where the extraction of the  $\Lambda n$  scattering lengths might be feasible are discussed.

**PACS.** 11.55.Fv Dispersion relations – 13.75.-n Hadron-induced low- and intermediate-energy reactions – 13.75.Ev Hyperon-nucleon interactions – 25.40.-h Nucleon-induced reactions

## 1 Introduction

The experimental information on the  $\Lambda N$  interaction at low energies is rather poor and, moreover, of rather limited accuracy [1]. Specifically, the available data do not allow a reliable determination of the  $\Lambda N$  low-energy ( $^1S_0$ ,  $^3S_1$ ) scattering parameters. Therefore, it has been suggested in the past to consider inelastic processes where the  $\Lambda N$  system is produced in the final state and to exploit the occurring final-state interaction for the extraction of those scattering parameters. With this aim in mind, we [2,3], but also other groups [4,5], have recently looked at the reaction  $pp \rightarrow K^+ \Lambda p$  which can be studied experimentally at the COSY facility in Jülich and where concrete experiments have been already performed [6,7,8,9,10].

In the present paper we want to investigate the prospects of utilizing another strangeness-production reaction, namely  $\gamma d \rightarrow K^+ \Lambda n$  [11,12,13,14,15,16,17,18,19,20], for the determination of the  $\Lambda N$  low-energy scattering parameters. In this case pertinent experiments have been announced already long time ago at CEBAF [21], but are also possible at ELSA in Bonn [22], at the present JLAB facility [23], and the future MAMI-C project in Mainz [24]. In this paper we want to discuss the differences and, in particular, the merits but also possible disadvantages of considering the photon-induced strangeness production. We also investigate the spin dependence of the production amplitude and identify those spin-dependent observables that need to be measured to enable a separation of the  $^1S_0$  and  $^3S_1$  partial waves. Finally, we present quantitative results within a model calculation for one of the observables in question in order to demonstrate the kind of signal one could expect in a concrete experiment.

In our previous papers [2,3] we developed a method for a quantitative study of the final-state interactions in production reactions with large momentum transfer such as, e.g.,  $pp \rightarrow K^+ \Lambda p$  or  $pp \rightarrow K^0 \Sigma^+ p$ . In general, the method can be applied when there is a strong interaction in one of the produced two-body subsystems, and in addition there are no other channels with near-by thresholds that couple strongly to that system. Also, the interaction in the other final two-body subsystems should be weak. Then it is possible to reconstruct the elastic two-body ( $\Lambda N$ , say) amplitude (or at least its threshold value – the scattering length) via the invariant mass dependence of the production amplitude in the region where the relative  $\Lambda N$  momentum is small. The idea is to separate the different momentum scales appearing in the problem. In fact there are three scales one has to deal with: by assumption—we look only at very strong final state interactions leading to large scattering lengths—a very small scale given by the inverse of the scattering length,  $1/a$ , of the relevant final-state interaction, the inverse range of forces in the case of the elastic scattering, which is usually larger than the former scale, and – the largest scale – the inverse range of the production operator. From the point of view of analytical properties of the amplitude the latter two scales are roughly given by the corresponding closest left hand singularities. It is clear then that in the case of elastic scattering the location of those singularities is determined by the mass of the exchanged meson, whereas for the production reaction it is fixed in most cases by the value of the required momentum transfer  $q$  [25]. The production amplitude itself is free of the left hand singularities of the elastic amplitude, but has the same right hand cut. Dispersion theory enables to factorize the left hand sin-

gularities from the elastic amplitude and to represent the production amplitude as a product (see Refs. [26,27,28])

$$A(s, t, m^2) = \exp \left[ \frac{1}{\pi} \int_{m_0^2}^{\infty} \frac{\delta(m'^2)}{m'^2 - m^2 - i0} dm'^2 \right] \times \Phi(s, t, m^2), \quad (1)$$

where the exponent contains the full information on the right hand singularities of the elastic amplitude and the remaining factor  $\Phi$  possesses only left hand singularities and, therefore, in case of large momentum-transfer reactions, is only weakly dependent on  $m^2$ , the invariant mass of the considered two-body subsystem, e.g. of  $\Lambda N$ . In Eq. (1)  $\delta$  is the elastic  $\Lambda N$  phase shift and  $m_0 = m_A + m_N$ .  $s$  and  $t$  are the total c.m. energy squared and the 4-momentum transfer (from one of the initial particles to the kaon) squared, respectively. In a more realistic situation when inelastic channels are present at higher energy (as is the case for  $\Lambda N$  due to the opening of the  $\Sigma N$  channel) one can write down a similar expression where the integration involves only the range where the final state interaction is strong [2]

$$A(m^2) = \exp \left[ \frac{1}{\pi} \int_{m_0^2}^{m_{max}^2} \frac{\delta(m'^2)}{m'^2 - m^2 - i0} dm'^2 \right] \times \tilde{\Phi}(m^2, m_{max}^2). \quad (2)$$

Here  $\tilde{\Phi}(m^2, m_{max}^2)$  is also a slowly varying function of  $m^2$  provided that  $\delta$  is sufficiently small in the vicinity of  $m_{max}$ . Neglecting the mass dependence of  $\tilde{\Phi}(m^2, m_{max}^2)$  the scattering length  $a_S$  in a specific partial wave  $S$  can be then expressed in terms of the differential partial production cross section  $\sigma_S$ :

$$a_S = \lim_{m^2 \rightarrow m_0^2} \frac{1}{2\pi} \left( \frac{m_A + m_N}{\sqrt{m_A m_N}} \right) \times \mathbf{P} \int_{m_0^2}^{m_{max}^2} dm'^2 \sqrt{\frac{m_{max}^2 - m^2}{m_{max}^2 - m'^2}} \times \frac{1}{\sqrt{m'^2 - m_0^2} (m'^2 - m^2)} \log \left\{ \frac{1}{p'} \left( \frac{d^2 \sigma_S}{dm'^2 dt} \right) \right\}. \quad (3)$$

A detailed analysis of the uncertainties of Eq. (3) has shown that the theoretical error of the extracted value for the scattering length is of the order of 0.3 fm [2]. Note, however, that a possible influence of meson-baryon interactions in the other two-body subsystems has not been explicitly included into this estimate so far—we will do this below.

In this paper we present results for another strangeness-production process that is a possible candidate for the extraction of the  $\Lambda N$  scattering length, namely  $\gamma d \rightarrow K^+ \Lambda n$ . This reaction satisfies formally the main condition needed for the dispersion integral method to be applied: The momentum transfer in this reaction is large compared to the typical range of the final state  $\Lambda N$  interaction. The required c.m. momentum of the initial photon

to produce the  $K \Lambda N$  system at threshold is around 600 MeV/c. However, in contrast to the  $NN$  induced reaction, here a new small scale might enter the reaction depending on the kinematics: for forward going kaons at sufficiently high energy the intermediate nucleon is off-shell only by the small binding energy of the deuteron before the photon couples. Then quasifree production dominates the reaction and the dispersion integral method cannot be applied anymore. Therefore, one has to impose additional kinematical conditions to ensure that quasifree production is not allowed or at least strongly suppressed.

In Sec. 2 we consider the spin structure of the reaction amplitude for  $\gamma d \rightarrow K^+ \Lambda n$  and we derive those spin observables that need to be measured in order to separate the  $\Lambda N$  spin-singlet and spin-triplet states. In Sec. 3 we estimate uncertainties of the extracted  $\Lambda N$  scattering length that could arise from the interaction in the other final states ( $K \Lambda$ ,  $KN$ ). Concrete results for the spin observable that projects on the spin-triplet state are presented in Sec. 4, based on a model calculation by Yamamura et al. [15]. Furthermore, as a test we apply the dispersion integral method described above to those specific model predictions for extracting the  $\Lambda n$   $^3S_1$  scattering length. We also discuss issues concerning the kinematical regions where experiments should be preferably performed in order to ensure a reliable determination of the scattering lengths. Specifically, we identify the kinematical conditions, where the quasifree production is not allowed or strongly suppressed and where then the dispersion integral method can be reliably applied. The paper closes with a brief Summary.

## 2 Spin observables

An important issue for the extraction of the low-energy scattering parameters is the separation of the different spin components in the  $\Lambda N$  system. In Ref. [2] we have shown that by measuring specific spin observables in the reaction  $NN \rightarrow NK \Lambda$  one can project on the production of spin-singlet or spin-triplet states. Let us now discuss what observables can be used to disentangle the different spin states for the reaction  $\gamma d \rightarrow K^+ \Lambda n$ .

We start from the general form for the matrix element of the process  $\gamma d \rightarrow K^+ \Lambda n$ :

$$M = A(\epsilon_d \cdot \epsilon_\gamma) + \mathbf{B} \cdot (\epsilon_d \times \epsilon_\gamma) + C^{(ij)} \left( \epsilon_d^i \epsilon_\gamma^j + \epsilon_d^j \epsilon_\gamma^i - \frac{2}{3} \delta^{ij} (\epsilon_d \cdot \epsilon_\gamma) \right), \quad (4)$$

where  $\epsilon_\gamma$  and  $\epsilon_d$  are the polarization vectors of the photon and deuteron, respectively. If we assume the  $\Lambda N$  system to be in an  $S$ -wave, then we have only the (normalized) initial momentum  $\hat{p}$  and the outgoing kaon momentum  $\mathbf{q}'$  available to construct the structures for the coefficients. If the final  $\Lambda N$  system is in a spin triplet state we have in addition  $\mathbf{S}'$ , the spin vector of the final state, that has to appear linearly in the coefficients  $A$ ,  $B$  and  $C$ . Parity conservation demands that both  $\hat{p}$  and  $\mathbf{q}'$  appear either

in an odd number or in an even number. Thus, we have for the spin singlet case:

$$\begin{aligned} A^s &= a^s, \\ \mathbf{B}^s &= b^s(\mathbf{q}' \times \hat{p}), \\ C^{(ij)s} &= c_1^s \hat{p}^i \hat{p}^j + c_2^s q'^i q'^j + c_3^s q'^i \hat{p}^j. \end{aligned} \quad (5)$$

On the other hand, for the spin triplet final state we get

$$\begin{aligned} A^t &= a^t \mathbf{S}' \cdot (\mathbf{q}' \times \hat{p}), \\ \mathbf{B}^t &= b_1^t \mathbf{S}' + (\mathbf{S}' \cdot \hat{p})(b_2^t \hat{p} + b_3^t \mathbf{q}') + b_4^t \mathbf{q}'(\mathbf{S}' \cdot \mathbf{q}') \\ C^{(ij)t} &= \mathbf{S}' \cdot (\mathbf{q}' \times \hat{p})(c_1^t \hat{p}^i \hat{p}^j + c_2^t q'^i q'^j + c_3^t q'^i \hat{p}^j) \\ &\quad + c_4^t \mathbf{S}'^i (\mathbf{q}' \times \hat{p})^j + (\mathbf{S}' \times \mathbf{q}')^i (c_5^t q'^j + c_6^t \hat{p}^j) \\ &\quad + (\mathbf{S}' \times \hat{p})^i (c_7^t q'^j + c_8^t \hat{p}^j). \end{aligned} \quad (6)$$

Note that the coefficients  $a^s$ ,  $b^s$ , etc. are functions of  $(\mathbf{q}')^2$  and  $\mathbf{q}' \cdot \hat{p}$ . A significant simplification allowing one to separate different spin states can be achieved if we assume  $\mathbf{q}'$  to be along the beam direction (in particular then  $\mathbf{B}^s$  and  $A^t$  vanish). This means that one considers the situation where the kaon is emitted either in forward or in backward direction. Then we can look at two different cases:

- $\epsilon_d \parallel \hat{p}$ . As real photons are transverse ( $\lambda_\gamma = \pm 1$ ),  $A^s$  and  $C^{(ij)s}$  do not contribute. Thus for real photons and longitudinal target polarization ( $\lambda_d = 0$ ), only the spin-triplet state contributes through  $b_1^t$  and  $C^{(ij)t}$ . Hence this is the case where we can study the spin-triplet final-state. The observable that provides access to the longitudinal target polarization is

$$(1 - \sqrt{2}T_{20}^0) \frac{d\sigma_0}{dm_{\Lambda n} d\Omega_q} \sim |b_1^t + c_8^t + (c_6^t + c_7^t)(\hat{p}\mathbf{q}) + c_5^t \mathbf{q}^2|^2, \quad (7)$$

where  $T_{20}^0$  is defined by

$$\begin{aligned} T_{20}^0 &= \sum_{\lambda_1, \lambda_2, \lambda_3} \Omega_{20; \lambda_1 \lambda_3} M_{\lambda_1 \lambda_2} M_{\lambda_3 \lambda_2}^* \\ &\quad / \sum_{\lambda_1, \lambda_2} M_{\lambda_1 \lambda_2} M_{\lambda_1 \lambda_2}^* \end{aligned} \quad (8)$$

with  $\lambda_1, \lambda_3$  being the deuteron spin projection onto the photon momentum and  $\lambda_2, \lambda_4$  the circular polarization of the photon. The operators  $\Omega_{ij}$  are defined by

$$\begin{aligned} \Omega_{10} &= \sqrt{\frac{3}{2}} \begin{pmatrix} 1 & 0 & 0 \\ 0 & 0 & 0 \\ 0 & 0 & -1 \end{pmatrix}, \quad \Omega_{20} = \sqrt{\frac{1}{2}} \begin{pmatrix} 1 & 0 & 0 \\ 0 & -2 & 0 \\ 0 & 0 & 1 \end{pmatrix}, \\ \Omega_{22} &= \sqrt{3} \begin{pmatrix} 0 & 0 & 1 \\ 0 & 0 & 0 \\ 0 & 0 & 0 \end{pmatrix}, \quad \Omega_{2-2} = \sqrt{3} \begin{pmatrix} 0 & 0 & 0 \\ 0 & 0 & 0 \\ 1 & 0 & 0 \end{pmatrix}, \\ \Omega^c &= \begin{pmatrix} 1 & 0 \\ 0 & -1 \end{pmatrix}, \quad \Omega^l = \begin{pmatrix} 0 & -1 \\ -1 & 0 \end{pmatrix}, \end{aligned} \quad (9)$$

see, e.g., Ref. [30]. A complete description of the polarization observables for such kind of reactions can be found in Ref. [31].

- $\epsilon_d \perp \mathbf{p}$ . In this case  $C^{(ij)t}$  vanishes, and the spin-singlet amplitudes (proportional to  $A^s$  and  $C^{(ij)s}$ ) are symmetric with respect to an interchange of  $\epsilon_d$  and  $\epsilon_\gamma$ , whereas the spin-triplet amplitude (proportional to  $\mathbf{B}^t$ ) is antisymmetric. This allows to construct combinations of spin observables containing only spin-singlet or spin-triplet contributions (two combinations for each spin), namely

$$\begin{aligned} &(2 + \sqrt{2}T_{20}^0 - \sqrt{3}(T_{22}^l + T_{2-2}^l)) \frac{d\sigma_0}{dm_{\Lambda n} d\Omega_q} \\ &= -\sqrt{3}(\sqrt{2}T_{10}^c + (T_{22}^l + T_{2-2}^l)) \frac{d\sigma_0}{dm_{\Lambda n} d\Omega_q} \\ &\sim \left| -a^s + \frac{2}{3}(c_1^s + c_3^s(\hat{p}\mathbf{q}) + c_2^s \mathbf{q}^2) \right|^2 \end{aligned} \quad (10)$$

$$\begin{aligned} &(2 + \sqrt{2}T_{20}^0 + \sqrt{3}(T_{22}^l + T_{2-2}^l)) \frac{d\sigma_0}{dm_{\Lambda n} d\Omega_q} \\ &= \sqrt{3}(-\sqrt{2}T_{10}^c + (T_{22}^l + T_{2-2}^l)) \frac{d\sigma_0}{dm_{\Lambda n} d\Omega_q} \\ &\sim |b_1^t + b_2^t + b_3^t(\hat{p}\mathbf{q}) + b_4^t \mathbf{q}^2|^2, \end{aligned} \quad (11)$$

with

$$\begin{aligned} T_{2\pm 2}^l &= \sum_{\lambda_1, \lambda_2, \lambda_3, \lambda_4} \Omega_{2\pm 2; \lambda_1 \lambda_3} \Omega_{\lambda_2 \lambda_4}^l M_{\lambda_1 \lambda_2} M_{\lambda_3 \lambda_4}^* \\ &\quad / \sum_{\lambda_1, \lambda_2} M_{\lambda_1 \lambda_2} M_{\lambda_1 \lambda_2}^* \\ T_{10}^c &= \sum_{\lambda_1, \lambda_2, \lambda_3, \lambda_4} \Omega_{10; \lambda_1 \lambda_3} \Omega_{\lambda_2 \lambda_4}^c M_{\lambda_1 \lambda_2} M_{\lambda_3 \lambda_4}^* \\ &\quad / \sum_{\lambda_1, \lambda_2} M_{\lambda_1 \lambda_2} M_{\lambda_1 \lambda_2}^*. \end{aligned} \quad (12)$$

Here the upper index ( $c$  or  $l$ ) refers to circularly or linearly polarized photons. Therefore, the only possibility to obtain a pure spin-singlet  $\Lambda N$  final-state is to perform a double polarization experiment.

### 3 Influence of the meson-baryon interaction

As mentioned in the Introduction, in the derivation of Eq. (3) we assumed that the interactions in the other two-body subsystems in the final state are small. This concerns the  $K\Lambda$  and the  $KN$  systems. The reason was that for excess energies in the order of 100 to 200 MeV, the kinetic energy in those subsystems is large and does not vary strongly with the relative  $\Lambda N$  momentum, when the latter system is considered near its threshold for the extraction of the  $\Lambda N$  scattering length, with the relative  $\Lambda N$  momentum, when the latter system is considered near its threshold for the extraction of the  $\Lambda N$  scattering length, and therefore the energy dependence of the production amplitude should not change significantly. It was noted, however, in [29] that one should still be cautious because of possible effects due to the presence of  $N^*$  resonances in the  $K\Lambda$  system. Therefore, in the following we are going to derive some qualitative estimates as to how large

the effect of such resonances can be for the extracted  $\Lambda N$  scattering length. Note that this issue is relevant for both reactions  $\gamma d \rightarrow KYN$  and  $pp \rightarrow KYN$ , although the details might differ. In particular the relative importance of contributions from resonances and of the background will depend on the specific reaction mechanisms. We assume here that the energy dependence of the production amplitude is modified by a factor

$$\Phi = \frac{1}{M_{\Lambda K}^2 - M_R^2 + i\Gamma_R M_R}, \quad (13)$$

averaged over the  $\Lambda N$  c.m. angle, i.e. we consider only the resonance contribution but neglect a background. Here  $M_R$  and  $\Gamma_R$  are the Breit-Wigner mass and width of the resonance, respectively. In general a nontrivial interference of the resonance amplitude with the background can produce a stronger mass dependence of the production amplitude. On the other hand the sum of all partial waves in the  $\Lambda K$  system will have the opposite effect. Therefore, we believe that the above approximation is reasonable in order to estimate the uncertainty in the extracted  $\Lambda N$  scattering length induced by the presence of resonances in the  $\Lambda K$  system. For simplicity we consider only an  $S$ -wave resonance. Expanding  $\Phi$  in terms of the  $\Lambda N$  c.m. momentum  $p$  one gets

$$\begin{aligned} \Phi &\approx \frac{1}{\Delta M^2 + i\Gamma_R M_R - Cp^2 - 2kpx} \\ &\approx \frac{1}{\Delta M^2 + i\Gamma_R M_R} \\ &\times \left( 1 + \frac{Cp^2 + 2kpx}{\Delta M^2 + i\Gamma_R M_R} + \frac{4k^2 p^2 x^2}{(\Delta M^2 + i\Gamma_R M_R)^2} \right), \end{aligned} \quad (14)$$

where  $C = 2 + \frac{m_\Lambda - m_n}{m_n} \left( \frac{s - m_K^2 - (m_\Lambda + m_n)^2}{2m_\Lambda(m_\Lambda + m_n)} + 1 \right)$ ,  $k$  is the kaon momentum in the c.m. system of  $\Lambda N$  (at  $p = 0$ ),  $x$  is the cosine of the angle between the kaon and  $\Lambda$  in the same system and

$$\begin{aligned} \Delta M^2 &= M_{\Lambda K}^2(p=0) - M_R^2 = m_K^2 + m_\Lambda^2 + \\ &\frac{(s - m_K^2 - (m_\Lambda + m_N)^2)m_\Lambda}{m_\Lambda + m_N} - M_R^2. \end{aligned} \quad (15)$$

Note that the factor  $C$  is of the order of 2 for the considered excess energies up to several hundred MeV because the mass difference between the  $\Lambda$  and nucleon is small. In order to estimate the effect that resonances may have on the extraction of the scattering length we evaluated the dispersion integral Eq. (3) for the amplitude given in Eq. (14). Corresponding results are shown in Fig. 1 as a function of the excess energy. Obviously, the resulting scattering length should be identical to zero if there is completely no influence. We see that the deviations due to such resonances are somewhat dependent on the excess energy but amount to  $\pm 0.2$  fm at most.

For a qualitative understanding of the role of the various scales it is instructive to proceed as follows. Averaging

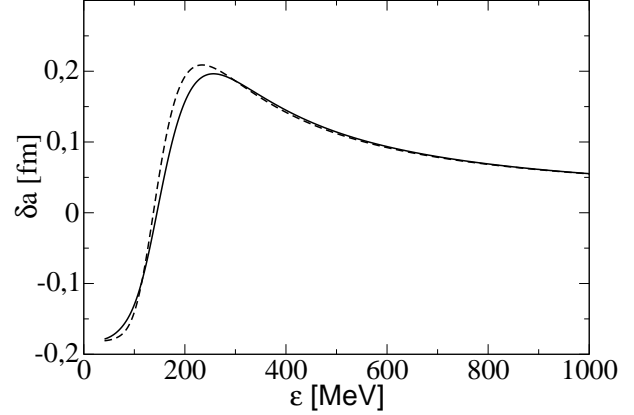


**Fig. 1.** Error in the extracted scattering length due to the presence of a resonance structure in the  $K\Lambda$  subsystem depending on the available excess energy  $\epsilon$ . The solid line shows the result of the dispersion integral while the dashed line corresponds to an approximation, cf. discussion in Sec. 3.

over  $x$  and removing a constant prefactor one obtains

$$\langle \Phi \rangle \sim 1 + \frac{Cp^2}{\Delta M^2 + i\Gamma_R M_R} + \frac{4k^2 p^2}{3(\Delta M^2 + i\Gamma_R M_R)^2}. \quad (16)$$

For the production amplitude squared one gets the following mass dependence

$$\begin{aligned} |A|^2 &\sim 1 + \frac{2Cp^2 \Delta M^2}{(\Delta M^2)^2 + \Gamma_R^2 M_R^2} \\ &+ \frac{8k^2 p^2 ((\Delta M^2)^2 - \Gamma_R^2 M_R^2)}{3((\Delta M^2)^2 + \Gamma_R^2 M_R^2)^2}. \end{aligned} \quad (17)$$

The corresponding contribution to the  $\Lambda N$  scattering length is (see Ref. [2])

$$\delta a \sim p_{max} \left[ \frac{C \Delta M^2}{(\Delta M^2)^2 + \Gamma_R^2 M_R^2} + \frac{4k^2 ((\Delta M^2)^2 - \Gamma_R^2 M_R^2)}{3((\Delta M^2)^2 + \Gamma_R^2 M_R^2)^2} \right], \quad (18)$$

where  $p_{max} \approx 200$  MeV/c reflects the limit of the dispersion integral. It is easy to see that the result depends on two important scales: the resonance width (typically 150–200 MeV) and  $\Delta M^2$  which is determined by the excess energy. In order to obtain a rough idea for the order of magnitude of the corrections to the scattering length let us put  $\Delta M^2 = 0$ . Then  $\delta a \sim -4k^2 p_{max} / (3\Gamma_R^2 M_R^2)$ . If we take as a typical example the mass of the resonance to be  $M_R = 1700$  MeV and its width to be  $\Gamma_R = 150$  MeV, then  $k \sim 400$  MeV/c, which yields  $\delta a \sim -0.1$  fm. The absolute value of  $\delta a$  becomes smaller as  $\Delta M^2$  increases. In Fig. 1 the result for  $\delta a$  calculated by means of Eq. (18) is compared to the value obtained from the full dispersion integral Eq. (3). The two curves turn out to be almost identical and, therefore, justify the use of our approximations made in Eqs. (14)–(18). We conclude that for such excess energies where the available phase space for the  $K\Lambda$

system covers the resonance region one has to expect an additional uncertainty of the extracted scattering length in the order of 0.2 fm—this has to be added to the one estimated previously leading to a total theoretical uncertainty of 0.5 fm. A more concrete quantitative statement can be made only by analyzing the actual experimental Dalitz plots, where one should clearly see whether there is a strong dependence of the production amplitude on the  $K\Lambda$  invariant mass or not.

## 4 Results and discussion

As already said in the Introduction, the reaction  $\gamma d \rightarrow K^+ \Lambda n$  satisfies formally the main condition needed for the dispersion integral method to be applied: The momentum transfer in this reaction is large compared to the typical range of the final state  $YN$  interaction. The required c.m. momentum of the initial photon to produce the  $YNK$  system at threshold is equal to 584 MeV/c. In order to be able to resolve the structure induced by the  $\Lambda N$  interaction one needs at least data covering  $\Lambda N$  invariant masses in the range of 40 MeV from the threshold, cf. Ref. [2]. In that work we argued also that the pertinent experiments should be performed preferably at somewhat higher total energies. Then there will be no distortion of the signal within that 40 MeV range by the (upper) limit of the available phase space. Moreover, effects from possible interactions in the other final states ( $KN$ ,  $K\Lambda$ ) are kinematically better separated and should not influence the results for  $\Lambda N$  too much.

An important kinematical constraint for the reaction  $\gamma d \rightarrow K^+ \Lambda n$  is the limitation of the kaon angle to very forward or very backward directions because only then a separation of the spin-singlet and spin-triplet states is possible, as shown in Sec. 2. Unfortunately, there are indications that the total count rate could be very small in the backward region. For example, the model calculation of Salam and Arenhövel [17] suggests that the cross sections drop dramatically in that angular range, cf. their Fig. 12. This can be easily understood within the impulse approximation. In this case the spectator nucleon carries necessarily a large momentum for kaons produced in backward direction and for such large momenta the deuteron wave function is strongly suppressed. Additional production mechanisms that involve two-step processes, considered also in Ref. [17], relax the situation somewhat. But still it could be difficult to perform measurements for the backward region and one has to wait for concrete experiments in order to see whether sufficient statistics can be achieved.

Therefore, in the following we will concentrate on results for forward angles. However, in this case there is a particular singularity of the production amplitude that imposes some restrictions on the application of our method. It is the so-called quasi-free production mechanism (see Fig. 2). When the available excess energy in the  $\Lambda n K^+$  system is around 90 MeV or more then the production of the  $\Lambda K^+$  system is possible on a single proton, resting in the deuteron rest frame. Therefore, this effect introduces a

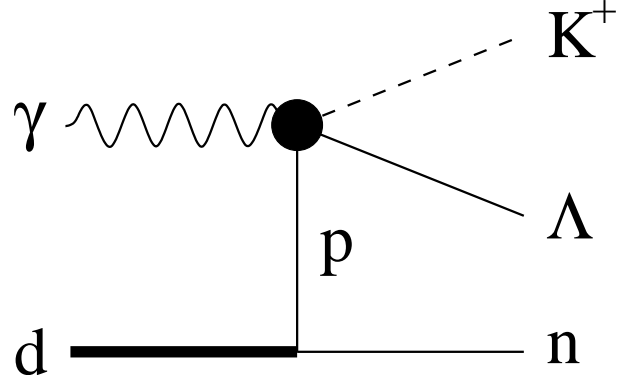


**Fig. 2.** Diagram corresponding to the quasi-free kaon production on the proton.

new, very small scale in the production operator caused by the small deuteron binding energy. It is clear that this particular production mechanism is dominant when the relative momentum of the two nucleons inside the deuteron is not large. Thus, it influences primarily forward kaons where then the  $\Lambda N$  system is moving in direction of the deuteron momentum in the c.m. system. Note that the peak is shifted somewhat away from very low relative  $YN$  momenta because the photon cannot produce a  $\Lambda$  at rest on a proton at rest.

In Fig. 3 we demonstrate the situation for a concrete model calculation where results for  $1 - \sqrt{2}T_{02}^0$  at  $E_\gamma = 1300$  MeV ( $\epsilon = 349$  MeV) are shown for kaon production in forward direction ( $\Theta_K = 0^\circ$ ). Details of the model calculation can be found in Ref. [15]. Let us mention here that the calculation is done in the impulse approximation including the  $YN$  final-state interaction, utilizing the deuteron wave function of the Nijmegen93 potential [32] and the NSC97f  $YN$  force [33]. The elementary kaon-production amplitude on the nucleon ( $\gamma N \rightarrow K\Lambda$ ) is derived from a set of tree-level Feynman diagrams where the free parameters have been fixed so that all available  $K^+\Lambda$ ,  $K^+\Sigma^0$ , and  $K^0\Sigma^+$  photoproduction data in the relevant energy region are reproduced [34]. Additional production mechanisms involving, e.g.,  $KN$  rescattering or the  $\pi N \rightarrow K\Lambda$  process, considered in Ref. [17], are not included in this model. However, those mechanisms contribute predominantly for kaon production at backward angles [17] and are not so important for the forward angles we consider.

The model calculation presented in Fig. 3 clearly shows the presence of a bump due to quasi-free kaon production. It occurs at fairly small  $\Lambda n$  invariant masses and, therefore, makes a reliable determination of the  $\Lambda n$  scattering length from data impossible. Thus, for extracting the  $\Lambda n$  scattering length from forward-angle data one has to consider the reaction  $\gamma d \rightarrow K^+ \Lambda n$  for energies below the appearance of this quasi-free peak, i.e. at excess energies 40 – 50 MeV. First of all one should note that the influence of the  $\Lambda K$  interaction is not necessarily much stronger than at higher excess energies, since we are within the resonance region in both cases. Therefore, the uncertainty of the method remains the same. This issue was

addressed already in the previous section. Another problem is the limited phase space at low excess energies. The phase space is proportional to  $q' \times p' \times dm_{\Lambda n}$ . Since we are interested in the region of small relative momenta  $p'$  in the  $\Lambda n$  system in any case the suppression enters only due to the factor  $q'$ . The concrete effect of the suppression depends, of course, on the actual shape of the mass spectrum, but to get a rough estimate one can compare the  $q'$  values for different excess energies at the  $\Lambda n$  threshold ( $p' = 0$ ). For example, for the excess energy 50 MeV this value is about 2.5 times smaller than for 300 MeV. This means that the suppression is not such a serious problem in our case.

mechanism remains dominant even at low energies). In a pure  $S$  wave situation the allowed operator structure given in Eqs. (5,6) simplifies significantly and, in particular, the reaction amplitude does not depend on the direction of the kaon momentum anymore. Consequently, all expressions in Sec. 2 are valid for arbitrary angles. Therefore, one can work with observables integrated over the kaon angle in the c.m. system which means that a significant enhancement of the experimental statistics can be achieved. In addition the angular integration allows to get rid of interference terms between the  $S$ - and (small)  $P$ -waves that depend linearly on the kaon momentum so that possible influences from the energy dependence of the production operator, which is primarily due to terms linear in  $q'$ , are minimized.

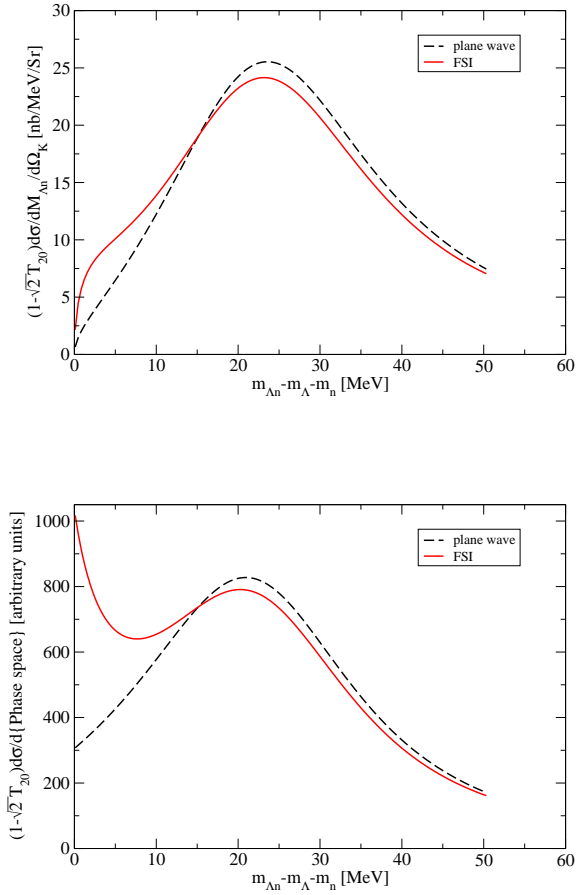


**Fig. 3.** Top: Model results for the spin-dependent observable  $1 - \sqrt{2}T_{02}^0$  at  $E_\gamma = 1300$  MeV and  $\Theta_K = 0^\circ$  as a function of the  $\Lambda n$  invariant mass  $m_{\Lambda n}$ . The dashed line is the impulse approximation while the solid line is the full result including the  $\Lambda n$  final-state interaction. Bottom: Same results but the phase-space factor is divided out.

An interesting side aspect at low excess energies is that then also the kaons should be predominantly produced in an  $S$ -wave relative to the  $\Lambda n$  system (unless the quasifree

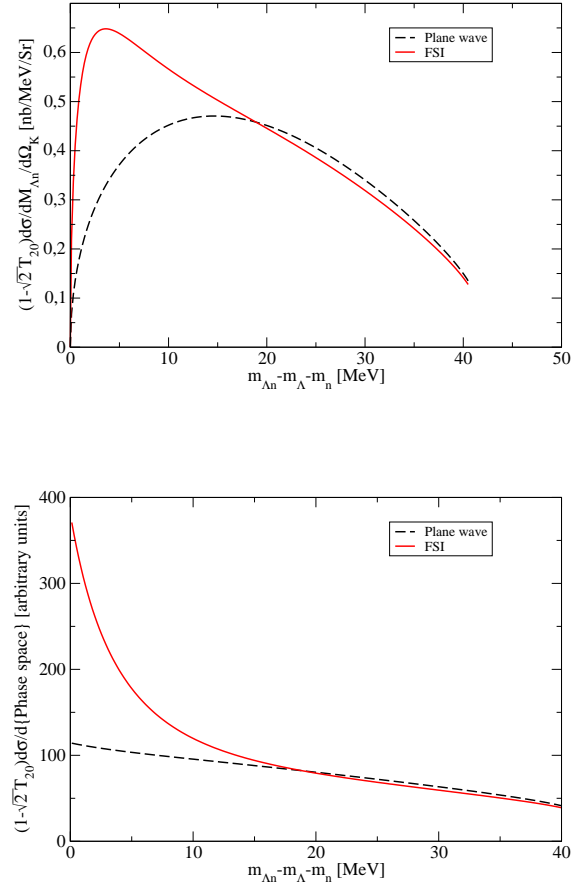


**Fig. 4.** Top: Model results for the spin-dependent observable  $1 - \sqrt{2}T_{02}^0$  at  $E_\gamma = 850$  MeV and  $\Theta_K = 0^\circ$  as a function of the  $\Lambda n$  invariant mass  $m_{\Lambda n}$ . The dashed line is the impulse approximation while the solid line is the full result including the  $\Lambda n$  final-state interaction. Bottom: Same results but the phase-space factor is divided out.

In Fig. 4 we show predictions of the model calculation [15] for the spin observable  $1 - \sqrt{2}T_{02}^0$  for  $E_\gamma = 850$  MeV ( $\epsilon = 41.5$  MeV) and forward kaons. The dashed line is the result for the impulse approximation while the solid line corresponds to the full model including the  $\Lambda N$  FSI. It is obvious how strongly the  $\Lambda N$  interaction modifies the observable for invariant masses close to the  $\Lambda N$  threshold. When applying the dispersion integral method to this observable, cf. Ref. [2] for details, we obtain the scattering length of  $-2.06$  fm for the  $^3S_1$  partial wave. This has to be compared with  $a_t = -1.70$  fm of the  $YN$  model [33] used for the model calculation. Thus, the extracted scattering length differs from the one utilized in the model calculation by about  $0.4$  fm, which is in line with the uncertainty that is expected for the method [2]. Specifically, one has to keep in mind that the present model calculation includes also the uncertainties discussed in Sec. 3 because it is based on an elementary kaon-production amplitude that involves resonances in the  $AK$  channel [34].

## 5 Summary

In the present paper we have studied the prospects of utilizing the strangeness-production reaction  $\gamma d \rightarrow K^+ \Lambda n$  for the determination of the  $\Lambda n$  low-energy scattering parameters. In particular, we derived those spin observables that need to be measured in order to isolate the  $\Lambda n$  singlet ( $^1S_0$ ) and triplet ( $^3S_1$ ) states, and we presented concrete results for one of those observables based on a model calculation by Yamamura et al. [15].

It turned out that a separation of the singlet and triplet states is feasible for experiments with kaons emitted either in forward or backward direction. On the other hand we found that the quasi-free production process, which dominates the reaction in forward direction at higher energies ( $E_\gamma \geq 900$  MeV/c), distorts the  $\Lambda N$  invariant mass spectrum so strongly that this particular kinematics cannot be used to extract the  $\Lambda N$  scattering lengths reliably. However, the situation looks very promising for experiments for energies just below the appearance of this quasi-free peak ( $E_\gamma \approx 850$  MeV/c). For this kinematics we presented a test calculation where we generated the required spin observables from the model of Yamamura et al. [15] and then we applied to them the dispersion integral method for extracting the  $\Lambda n$  scattering length. The value obtained for the  $^3S_1$  scattering length differs from the one utilized in the model calculation by about  $0.4$  fm, i.e. lies within the uncertainty that is expected for the method [2]. A determination of the scattering lengths is also possible from data at backward angles at any energy. However, for backward kaon production all model calculations predict rather small count rates. Thus, one was to wait for concrete experiments in order to see whether sufficient statistics can be achieved for this kinematics.

The presented estimation of the uncertainties of the extracted  $\Lambda N$  scattering length that could arise from the interaction in the other final states ( $K\Lambda$ ,  $KN$ ), together with the results of a concrete application, implies that the reaction  $\gamma d \rightarrow K^+ \Lambda n$  could allow to determine the

$\Lambda N$  scattering lengths with an accuracy similar to the reaction  $pp \rightarrow K^+ \Lambda p$ . Thus, we believe that the photon-induced reaction is an interesting alternative for extracting the  $\Lambda N$  scattering lengths and it is also very useful for cross-checking results obtained from the purely hadronic strangeness production.

## Acknowledgments

A.G. thanks the Institut für Kernphysik at the Forschungszentrum Jülich for its hospitality during the period when the present work was carried out. Furthermore, he would like to acknowledge financial support by the grant No. 436 RUS 17/75/04 of the Deutsche Forschungsgemeinschaft and by the Russian Fund for Basic Research, grant No.06-02-04013.

## References

1. G. Alexander et al., Phys. Rev. **173**, 1452 (1968).
2. A. Gasparyan, J. Haidenbauer, C. Hanhart, and J. Speth, Phys. Rev. C **69**, 034006 (2004).
3. A. Gasparyan, J. Haidenbauer, and C. Hanhart, Phys. Rev. C **72**, 034006 (2005).
4. J. T. Balewski et al., Eur. Phys. J. A **2**, 99 (1998).
5. F. Hinterberger and A. Sibirtsev, Eur. Phys. J. A **21**, 313 (2004).
6. J. T. Balewski et al., Phys. Lett. **B 420**, 211 (1998).
7. R. Bilger et al., Phys. Lett. **B 420**, 217 (1998).
8. S. Sewerin et al., Phys. Rev. Lett. **83**, 682 (1999).
9. P. Kowina et al., Eur. Phys. J. A **22**, 293 (2004).
10. S. Abd El-Samad et al., Phys. Lett. **B 632**, 27 (2006).
11. F.M. Renard and Y. Renard, Nucl. Phys. **B1**, 389 (1967).
12. B.O. Kerbikov, B.L.G. Bakker, and R. Daling, Nucl. Phys. **A480**, 585 (1988); B.O. Kerbikov, Phys. Atom. Nucl. **64**, 1835 (2001).
13. R.A. Adelseck and L.E. Wright, Phys. Rev. C **39**, 580 (1989).
14. X. Li and L.E. Wright, J. Phys. G **17**, 1127 (1991).
15. H. Yamamura, K. Miyagawa, T. Mart, C. Bennhold, H. Haberzettl, and W. Glöckle, Phys. Rev. C **61**, 014001 (1999).
16. O.V. Maxwell, Phys. Rev. C **69**, 034605 (2004); Phys. Rev. C **70**, 044612 (2004).
17. A. Salam and H. Arenhövel, Phys. Rev. C **70**, 044008 (2004).
18. K. Miyagawa, T. Mart, C. Bennhold, and W. Glöckle, Phys. Rev. C **74**, 034002 (2006) [arXiv:nucl-th/0608052].
19. A. Salam, K. Miyagawa, T. Mart, C. Bennhold, and W. Glöckle, Phys. Rev. C **74**, 044004 (2006) [arXiv:nucl-th/0608053].
20. J. M. Laget, Phys. Rev. C **75**, 014002 (2007) [arXiv:nucl-th/0603009].
21. B.L. Berman et al., CEBAF proposal PR-89-045 (1989).
22. V. Kleber and H. Schmieden, private communication.
23. P. Nadel-Turoński et al., JLAB proposal PR-06-103 (2006), [http://www.jlab.org/exp\\_prog/proposals/06/PR-06-103.pdf](http://www.jlab.org/exp_prog/proposals/06/PR-06-103.pdf)
24. R. Beck and A. Starostin, Eur. Phys. J. A **S19**, 279 (2004); R. Beck, Prog. Part. Nucl. Phys. **55**, 91 (2005).

- 25. C. Hanhart, Phys. Rept. **397** (2004) 155
- 26. N. I. Muskhelishvili, *Singular Integral Equations*, (P. Noordhoff N. V., Groningen, 1953).
- 27. R. Omnes, Nuovo Cim. **8**, 316 (1958).
- 28. W. R. Frazer and J. R. Fulco, Phys. Rev. Lett. **2**, 365 (1959).
- 29. A. Sibirtsev, J. Haidenbauer, H. W. Hammer, and S. Krewald, Eur. Phys. J. A **27**, 269 (2006).
- 30. Gerald G. Ohlsen, Rep. Prog. Phys. **35**, 717 (1972).
- 31. H. Arenhövel and A. Fix, Phys. Rev. C **72**, 064004 (2005).
- 32. V.G.J. Stoks, R.A.M. Klomp, C.P.F. Terheggen, and J.J. de Swart, Phys. Rev. C **49**, 2950 (1994).
- 33. Th.A. Rijken, V.G.J. Stoks, and Y. Yamamoto, Phys. Rev. C **59**, 21 (1999).
- 34. C. Bennhold, T. Mart, A. Waluyo, H. Haberzettl, G. Penner, T. Feuster, and U. Mosel, nucl-th/9901066.